ELSEVIER

Marine Geology 244 (2007) 93–108

MARINE GEOLOGY
INTERNATIONAL JOURNAL OF MARINE GEOLOGY, GEOCHEMISTRY AND GEOPHYSICS

www.elsevier.com/locate/margeo

Arctic Ocean record of last two glacial-interglacial cycles off North Greenland/Ellesmere Island — Implications for glacial history

N. Nørgaard-Pedersen [a,*], N. Mikkelsen [a], Y. Kristoffersen [b]

[a] *Geological Survey of Denmark and Greenland, DK-1350 Copenhagen, Denmark*
[b] *Department of Earth Science, University of Bergen, N-5007 Bergen, Norway*

Received 9 February 2007; received in revised form 13 June 2007; accepted 19 June 2007

Abstract

A sediment record from the practically unknown southernmost part of the Lomonosov Ridge off North Greenland/Ellesmere Island has been studied. GreenICE core 10 encompasses marine isotope stages (MIS) 7-1 and reveals changing paleoceanographic conditions and land-ocean connections during the last two glacial-interglacial cycles. The isotope record of planktic foraminifera *Neogloboquadrina pachyderma* (s) show large similarities to other Arctic Ocean key records, supporting that the pattern reflect over-regional changes of the halocline structure. The relatively low $\delta^{18}O$ values of subpolar foraminifera *Turborotalita quinqueloba* in the last interglacial unit support that the specimens represent local production, related to warm interglacial conditions and a reduced sea ice cover in the interior Arctic Ocean. Enhanced deposition of coarse ice-rafted debris took place during the MIS 8/7 transition, periods of MIS 6, MIS 6/5 transition, MIS 5d, MIS 4, and late MIS 3 (30–40 ^{14}C kyr BP). In MIS 2, IRD flux was low in the area. The IRD contains detrital carbonate similar to other Amerasia Basin records. The occurrence of fine-grained, calcite-rich detrital carbonate layers at glacial-interglacial transitions, seems unique to this area. We suggest that detrital carbonate was transported and deposited from nepheloid flows during deglaciations of Ellesmere Island, when the Atlantic Water boundary current along the continental margin was gaining strength.
© 2007 Elsevier B.V. All rights reserved.

Keywords: Arctic Ocean; Late Quaternary; Paleoceanography; oxygen isotope; IRD; detrital carbonate

1. Introduction

The present study focuses on a late Quaternary sediment core raised from the GreenICE drift camp in 2004 from a practically unknown region of the Arctic Ocean on the southernmost part of the Lomonosov Ridge north of Greenland/Ellesmere Island. The area, today, is characterised by the most severe ice conditions of the Arctic Ocean, hitherto hindering ice breaker navigation. Beyond the last glacial maximum, very little is known about the extension of ice sheets in Arctic Canada and northern Greenland (Funder and Hansen, 1996; Dyke et al., 2002; England et al., 2006; Polyak et al., 2007). The GreenICE core from adjacent to the continental margin shows a stratigraphically well-constrained record that can assist in identifying past periods of major regional glacial activity in the area.

A first study of the core material focused on the chronostratigraphic framework and detailed investigations of last interglacial conditions based on planktic foraminifera assemblages (Nørgaard-Pedersen et al., 2007). In this study we focus on the glacial-interglacial record of the last c. 240,000 years (MIS 7-1) in the

* Corresponding author. Tel.: +45 38142361; fax: +45 38142050.
E-mail address: nnp@geus.dk (N. Nørgaard-Pedersen).

0025-3227/$ - see front matter © 2007 Elsevier B.V. All rights reserved.
doi:10.1016/j.margeo.2007.06.008

longest core 10. We have obtained an almost complete oxygen and isotope record of *Neogloboquadrina pachyderma* (s) and present additionally isotope data on the subpolar species *Turborotalita quinqueloba* in last interglacial sediments. Moreover, by the detailed study of grain size distribution, geochemistry, and mineralogical data we intend to pinpoint possible source areas and timing of ice-rafted debris deposition and deglaciation events. Finally, we attempt to correlate specific events with other Arctic Ocean key records.

2. Geological and oceanographic setting

In May 2004, the GreenICE ice camp was deployed near the shallowest part of the Lomonosov Ridge (about 500 m) ca. 170 km north of Ellesmere Island (Fig. 1). During three weeks, the station drifted about 60 km towards the west, into water depths of about 1100 m. In addition to sea ice studies, sediment gravity coring and single channel reflection seismics were performed along the drift line over the broadly sloping margin of the Lomonosov Ridge (Kristoffersen and Mikkelsen, 2006; Nørgaard-Pedersen et al., 2007).

A passage with a minimum water depth of about 1150 m, separates the quite shallow (<500 m) southern part of the Lomonosov Ridge from the Lincoln Sea continental margin, north of Greenland/Ellesmere Island. The reflection seismic results show that about 1 km of sediments is found at the study site (Kristoffersen and Mikkelsen, 2006). The top of southern Lomonosov Ridge 50 km to the east is bevelled (550 m water depth) and only thin sediments (<50 ms ~45±5 m) cover acoustic basement. Erosion and/or non-deposition of sediment on the top of the Lomonosov Ridge contrasts with the presence of about 400 m thick hemipelagic sediment drape observed over the central Lomonosov Ridge (ACEX Shipboard Scientific Party, 2005). The flat bathymetry and thin sediment cover may imply glacial erosion by an ice shelf or deep draft icebergs during one or several periods of the Quaternary. Stronger boundary currents (especially during interglacials) may also have caused winnowing of fines and much reduced sedimentation rates.

The Lincoln Sea and the adjacent Arctic Ocean have the thickest sea ice cover of the entire Arctic Ocean, with mean ice thicknesses of 4 m or more (Wadhams, 1997; Wadhams and Davis, 2000; Haas et al., 2006). Icebergs are rare, but a relatively small ice shelf off northern Ellesmere Island occasionally releases large bergs to the Arctic Ocean. The present ice drift and surface water circulation over the study area either recirculate in the Beaufort Gyre over the Canada Basin or bend off towards the east with the Transpolar Drift Current when approaching the north Greenland shelf (Fig. 1). Below the cold, low salinity (31–32 psu) Arctic surface water layer, relatively warm (>0 °C) and saline (34.75 or greater) modified Atlantic Water flows as a boundary current counter clockwise around the Arctic Ocean continental margin, forming additional loops within the Arctic Ocean sub-basins (Rudels et al., 1999). Most of the Atlantic water mass probably follows the passage between Lincoln Sea and Lomonosov Ridge, thereby contributing to the intermediate water exchange between the Amerasia and the Eurasia Basin. However, a loop of Atlantic Water becomes detached from the continental margin off Ellesmere Island and flows northwards across the GreenICE site along the Lomonosov Ridge (Rudels et al., 1999; Kristoffersen and Mikkelsen, 2006).

3. Materials and methods

The present study focuses on the 1.76 m long gravity core, GreenICE core 10, taken at ca. 84° 48′ N, 74° 17′ W, at 1040 m water depth, (Fig. 1). Several shorter cores were recovered during the drift from about 500 m to 1100 m water depth, and these cores all correlate visually with the upper stratigraphic units (0.5 m) of core 10 (c.f. Nørgaard-Pedersen et al., 2007). Core 10 consists of alternating dark brown (10YR 6/3 and 10YR 4/4) and light yellowish grey/brown (2.5Y 6/2 and 2.5Y 6/4) beds of clayey and sandy mud with occasional occurrence of dropstones, up to several cm in diameter (Fig. 2). For descriptive purposes we use a simplified lithostratigraphy counting 'brown' (B) and 'light-coloured' (L) beds from top to bottom (Fig. 2). The brown beds are bioturbated silty clays rich in calcareous microfossils such as planktic and benthic foraminifera, ostracods and nannofossils. Light-coloured beds range from silty clays to sandy silts with occasional granule to small pebble-sized IRD and a sparse microfossil content. Semi-consolidated carbonate nodules are found in some of the light-coloured beds.

The core sections were X-rayed and split in two halfs, and magnetic susceptibility was measured with a Barthington MS2E1 probe on the split core in 1 cm steps. Subsamples of 3–4 cm^3 were taken every 1–2 cm down core. The samples were freeze-dried, weighed, and wet-sieved (>63 μm, >1 mm). The occurrence of IRD clasts with a diameter >5 mm ("dropstones") was noted during core description (incl. X-ray photos) and later subsampling of core sections. On selected IRD-rich sections, IRD lithologies of the >1 mm particles were determined semiquantitatively (in most cases <100 particles available). In addition to the >63 μm record based on wet sieving, detailed grain size measurements were performed

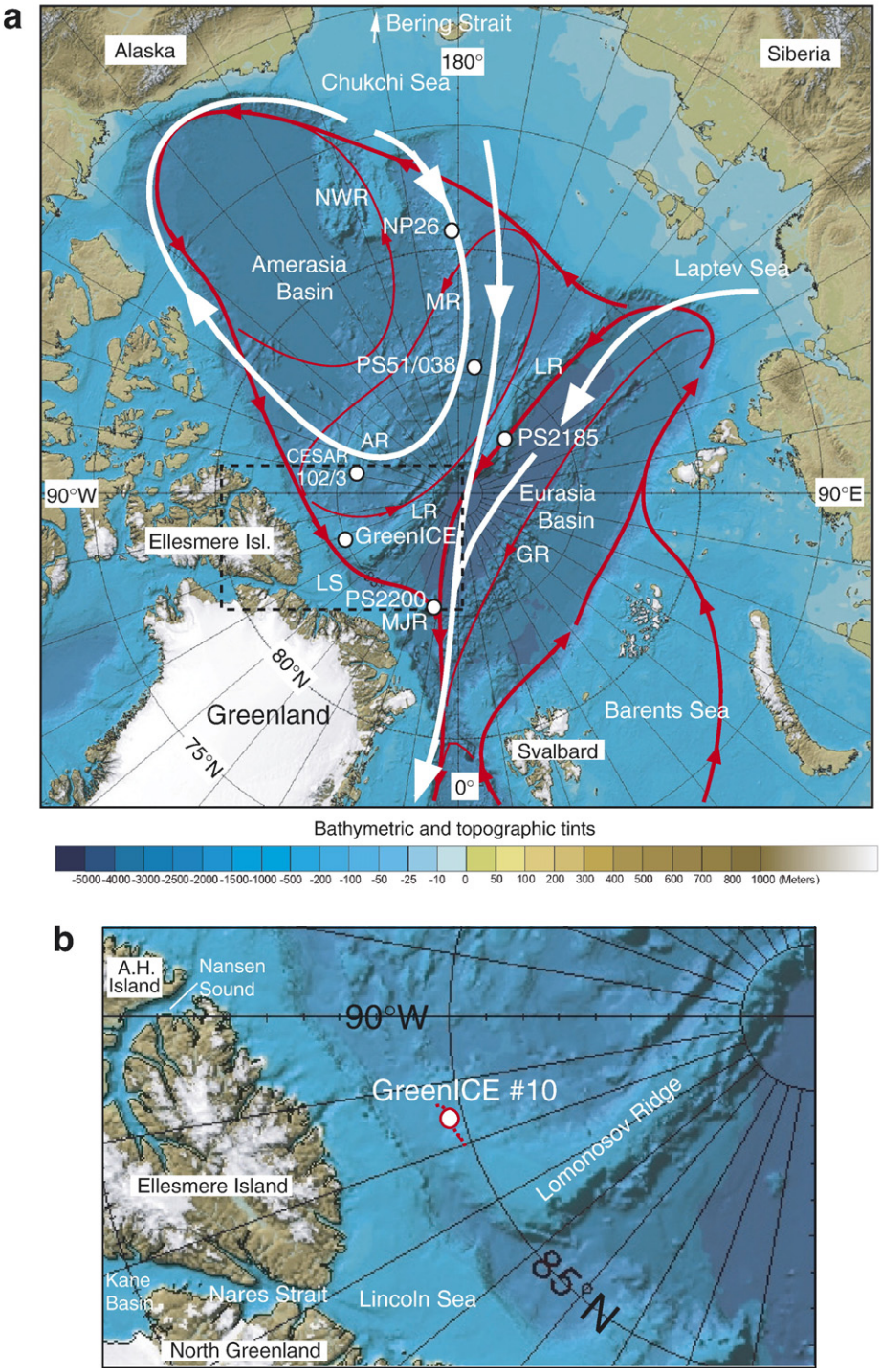


Fig. 1. (a) Arctic Ocean bathymetry, major surface currents (white), subsurface Atlantic Water circulation system (red), and location of GreenICE core 10 (square: detailed map in (b)). Other core sites mentioned in text, are also shown. LS: Lincoln Sea, LR: Lomonosov Ridge, MJR: Morris Jesup Rise, GR: Gakkel Ridge, AR: Alpha Ridge, MR: Mendeleev Ridge, NR: Northwind Ridge. (b) Detailed bathymetric map showing the drift track of the GreenICE station (dotted line) and location of coring site GreenICE #10 at a depth of 1040 m. A.H. Island: Axel Heiberg Island. Map source: International Bathymetric Chart of the Arctic Ocean (IBCAO).

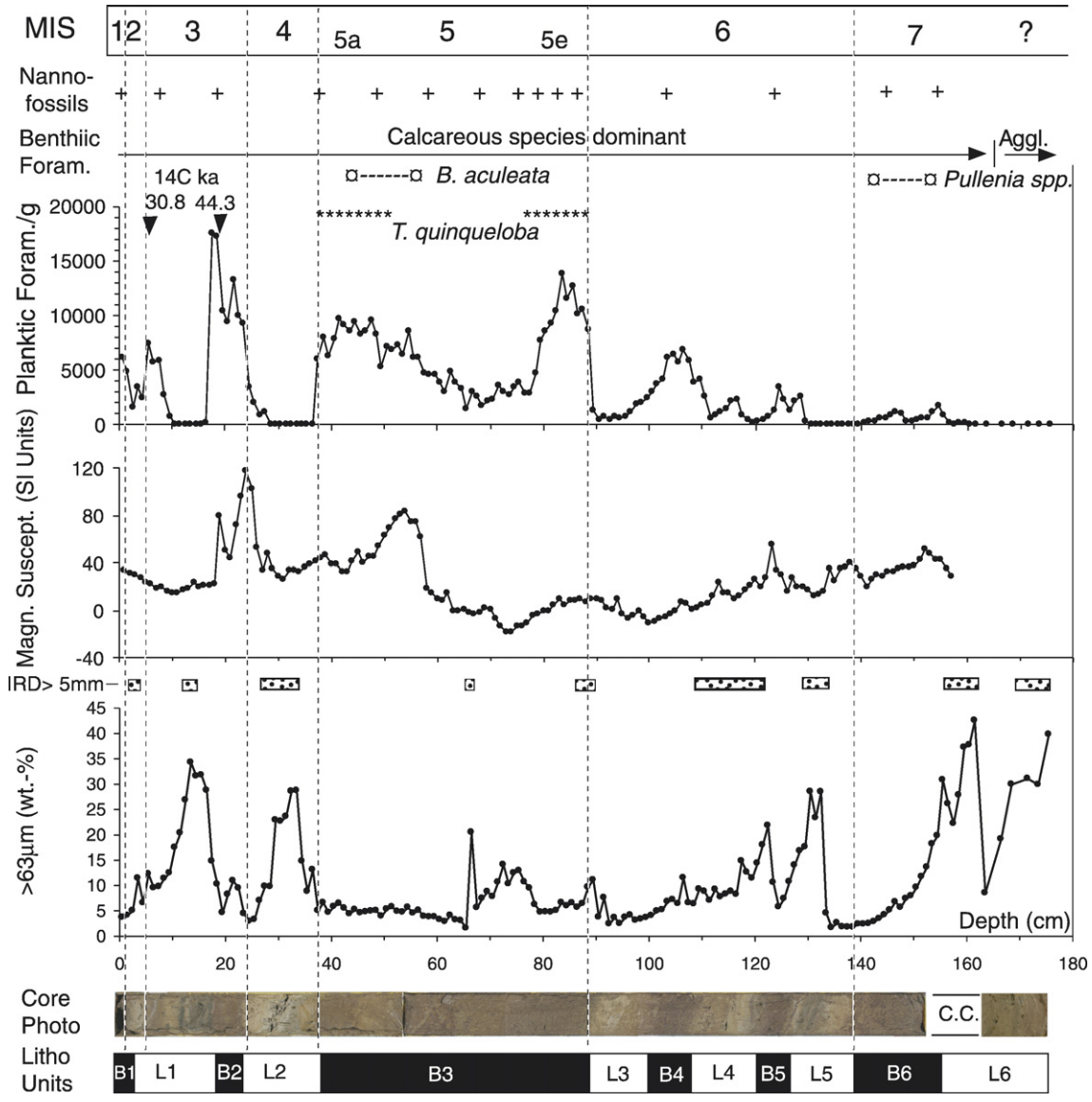


Fig. 2. GreenICE core 10 lithostratigraphic and chronostratigraphic data based on Nørgaard-Pedersen et al. (2007): Litho-units, core photo, coarse fraction content >63 µm, occurrence of IRD dropstones >5 mm, magnetic susceptibility, planktic foraminifera abundance (>63 µm). The stratigraphic levels with peak occurrence of subpolar planktic foraminifera *T. quinqueloba*, benthic foraminifera *Bulimina aculeata* and *Pullenia* spp, AMS-^{14}C dates, and nannofossils are indicated. The sediment stratigraphy in the cone below the core catcher (c.c.) in core 10 was intact. Marine isotope stages (MIS) 1-7 subdivision is based on further data in Nørgaard-Pedersen et al. (2007).

every 5–10 cm by a Malvern Mastersizer 2000 laser particle size analyser. The fraction 0.3–1700 µm was analysed and the cumulative volume-% determined for about 62 specific grain size intervals. The mean particle size and the weighted average of the sortable silt fraction (10–63 µm) was calculated (cf. McCave et al., 1995).

Oxygen and carbon isotopes were measured on planktic foraminifera *N. pachyderma* (s) from the 125–250 µm fraction (about 20 individuals per sample). In addition, oxygen and carbon isotopes were measured in the MIS 5e section on subpolar planktic foraminifera *T. quinqueloba* from the 63–125 µm fraction (about 80 individuals per sample). The isotope measurements were performed at the IFM-GEOMAR Research Center, Kiel.

Iron- (Fe_2O_3) and manganese oxides (MnO_2) were extracted from grounded bulk sediment samples by Na-citrate/Na-bicarbonate/Na-dithionite (Mehra and Jackson, 1960) and the amount of Fe and Mn were determined by Atomic Adsorption Spectroscopy (AAS). Total organic carbon (TOC) was measured from the CO_2 release after

dry combustion in a LECO-CS200 oven; these samples were first treated with 2 M HCl solution to remove $CaCO_3$ and washed several times with Millipore water to remove the Cl^{-1} ions. Total carbon (TC) was measured from the CO_2 release after dry combustion in a LECO-CS200 oven. $CaCO_3$ content was determined as: TC-TOC× 8.333. Relative calcium carbonate and dolomite content were determined on grounded bulk sediment samples by X-ray diffraction (XRD). The measurements were performed at GEUS on a Philips 1050 diffractometer with Co Kα radiation, β filter and pulse height selection, The measurements have been done as a continuous scan from 5–85° 2θ with a calculated stepsize of 0.1° 2θ (calculated time per step was 10 s). X-ray diffraction full pattern analyses were performed at selected $CaCO_3$-rich intervals at the ZEKAM laboratory, University of Bremen. The measurements were performed on a Philips X'Pert Pro multipurpose diffractometer equipped with a Cu-tube (k 1.541, 45 kV, 40 mA), a fixed divergence slit, a secondary monochromator and the X'Celerator detector system. The measurements were done as a continuous scan from 3–85° 2θ with a calculated step size of 0.016° 2θ (calculated time per step was 100 s). Mineral identification was done by means of the Philips software X'Pert HighScore™, which, besides the mineral identification, gives a semi-quantitative value for each identified mineral on the basis of Relative Intensity Ratio (R.I.R)-values. The R.I.R.-values are calculated as the ratio of the intensity of the most intense reflex of a specific mineral phase to the intensity of the most intense reflex of pure corundum (I/Ic) referring to the "matrix-flushing method" after Chung (1974).

The age model division into marine oxygen isotope stages (MIS) is based on AMS-^{14}C dates, nannofossil assemblages, benthic foraminifera marker beds (e.g. *Bulimina aculeata, Pullenia* spp.) and the occurrence of subpolar planktic foraminifera *T. quinqueloba*.

4. Results

4.1. Core stratigraphy

The lithostratigraphy and chronostratigraphy of GreenICE core 10 (Fig. 2) was presented in detail by Nørgaard-Pedersen et al. (2007). Two AMS ^{14}C dates at 5–6 cm (L1: 30.8 ^{14}C kyr BP) and 18–19 cm (B2: 44.3 ^{14}C kyr BP) indicate a MIS 3 age. The upper part of L1 (2–5 cm), poor in foraminifera and barren of nannofossils is assigned a MIS 2 age. Only about 2 cm of dark brown Holocene sediment (B1) was apparently preserved. Nannofossil data (Nørgaard-Pedersen et al., 2007) reveal that the thick brown B3 unit is dominated by *G. muellerae* with subordinate *E. huxleyi*, supporting a MIS 5 age (cf. Gard, 1988; Gard and Backman, 1990). An abundance peak of benthic foraminifera *B. aculeata* at 54-53 cm supports that the upper part of unit B3 corresponds to late MIS 5 (cf. Backman et al., 2004). The lower part of B3 (88–80 cm) is characterised by abundant subpolar *T. quinqueloba*, and this stratigraphic interval is assigned to the last interglacial (substage 5e) (Nørgaard-Pedersen et al., 2007). The light-coloured units between 140–90 cm (L5-L3) are enriched in IRD supporting dominantly glacial conditions, and this section is assigned to MIS 6. The occurrence of *Pullenia* spp. benthic foraminifera in the brown unit at 160–140 cm (B6) indicate a MIS 7 age. Thus, *Pullenia* spp. benthic foraminifers occur exclusively in the MIS 7 interval in Amerasia Basin and central Lomonosov Ridge cores (Jakobsson et al., 2001; Backman et al., 2004). The basal part of core 10 (L6) contains a transition upward from agglutinated benthic foraminifers to calcareous specimens. A similar faunal transition is well-known from a number of Arctic Ocean records (Poore et al., 1993; 1994; Jakobsson et al., 2001; Backman et al., 2004). For central Lomonosov Ridge records, Backman et al. (2004) infer that the agglutinated/calcareous faunal transition is close to the MIS 8/7 boundary. Moreover, as coccolith species *Emiliana huxleyi* are found in unit B6, it can be inferred that the basal sediment recovered is probably younger than (or equal to) late MIS 8, as its first evolutionary appearance is dated to about 0.26 Ma (Thierstein et al., 1977).

4.2. Oxygen and carbon isotope record

The δ^{18}O and δ^{13}C records of *N. pachyderma* (s) display pronounced variations with amplitudes exceeding those of the global ocean record (Fig. 3). The brown beds in general show intermediate to low δ^{18}O values (1–2‰) and relatively low δ^{13}C values (0–0.5‰). The light-coloured units, on the other hand, show relatively high δ^{18}O (2–3.5‰) and δ^{13}C (0.5–1.3‰) values. In the interior Arctic Ocean, we do not expect planktic oxygen isotope records to reveal an easily recognisable global ocean $\delta^{18}O_{water}$ pattern. The salinity-stratified nature of the Arctic Ocean and changes in the halocline structure related to variable river water/melt water flux and changes in the Atlantic Water and Pacific Water influx, bias the global isotopic pattern (Nørgaard-Pedersen et al., 2003; Polyak et al., 2004; Spielhagen et al., 2004). For this area, unusually high δ^{18}O values (4.0–4.6‰) stand out in the late MIS 4 section. Notably, this interval is characterised by peak $CaCO_3$ contents (>60%; mainly high-Mg calcite) and semi-consolidated

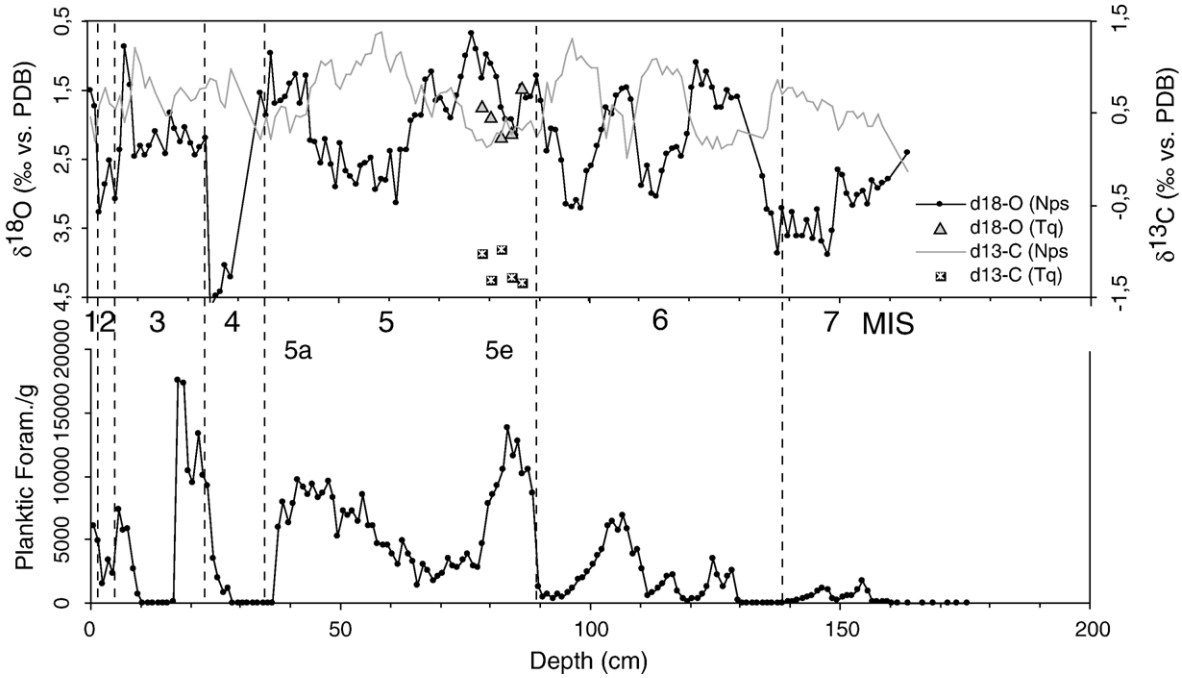


Fig. 3. Oxygen and carbon isotope (*N. pachyderma* (s)) and planktic foraminifera abundance record of GreenICE core 10. In the last interglacial section (MIS 5e), $\delta^{18}O$ and $\delta^{13}C$ values of subpolar planktic foraminifera *T. quinqueloba* are indicated to.

nodules. We cannot exclude that the special character of the sediment may have influenced the $\delta^{18}O$ values. High- $\delta^{18}O$ calcite-rich in-fill of *N. pachyderma* (s) chambers may have survived the pre-measurement cleansing process and thus have biased the results.

The *T. quinqueloba* $\delta^{18}O$ values appear to be very similar to the *N. pachyderma* (s) values in the MIS 5e unit and the low-high-low $\delta^{18}O$ pattern in the *N. pachyderma* (s) record is reproduced by the *T. quinqueloba* record (Fig. 3). $\delta^{13}C$ values of *T. quinqueloba*, however, are offset almost 1.5 permille lower than *N. pachyderma* (s) values. Such a species-dependant $\delta^{13}C$ offset is commonly observed between *T. quinqueloba* and *N. pachyderma* (s) (Volkmann and Mensch, 2001; Simstich et al., 2003).

4.3. Grain size distribution and IRD

The >63 μm fraction (wt.%) and the calculated mean particle size show similar down core trends (Fig. 4). Most of the samples show a broad modal peak at about 4–5 μm (fine silt) in the grain size distribution plots. Samples from the coarser-grained units in general show a bimodal distribution with a modal peak at about 5 μm and an additional secondary peak at about 100-500 μm (fine to coarse sand). The bimodal distribution is a common feature observed in glacial-marine sediments. Sea–ice rafted sediments are mostly fine-grained silts and clays, whereas ice-rafted debris melting out from icebergs includes more sand and coarser material (Clark and Hanson, 1983). Based on the grain size distribution plots and the sortable silt data, only the samples at 15-16 cm and 130–131 cm showing peak sortable silt weighted average values, may indicate short, episodal stronger bottom currents (cf. McCave et al., 1995).

The grain size and IRD >5 mm records (Figs. 2, 4) reveal enhanced deposition of coarse ice-rafted debris during the MIS 8/7 transition (basal part of core), early part of MIS 6, MIS 6/5 transition, MIS 5d, during MIS 4, and late MIS 3 (30–40 ^{14}C ka). IRD is sparse in the MIS 2 interval, but a few coarse erratics in this otherwise fine-grained interval indicate occasional IRD deposition. Based on semiquantitative analyses, quartz, detrital carbonate, sandstone, and metamorphic rock fragments are the most abundant IRD lithologies. Small pebbles of dark grey carbonate rock are common in the MIS 4 unit, also containing abundant fine-grained detrital carbonate in the upper part. Noteworthy, the basal part of core 10, representing the MIS 8/7 transition, show IRD enriched in siliceous rocks with almost no detrital carbonate.

4.4. Manganese and iron content

The MnO_2 content varies between 0.01 and 0.6% (Fig. 5). Low values are evidently associated with the

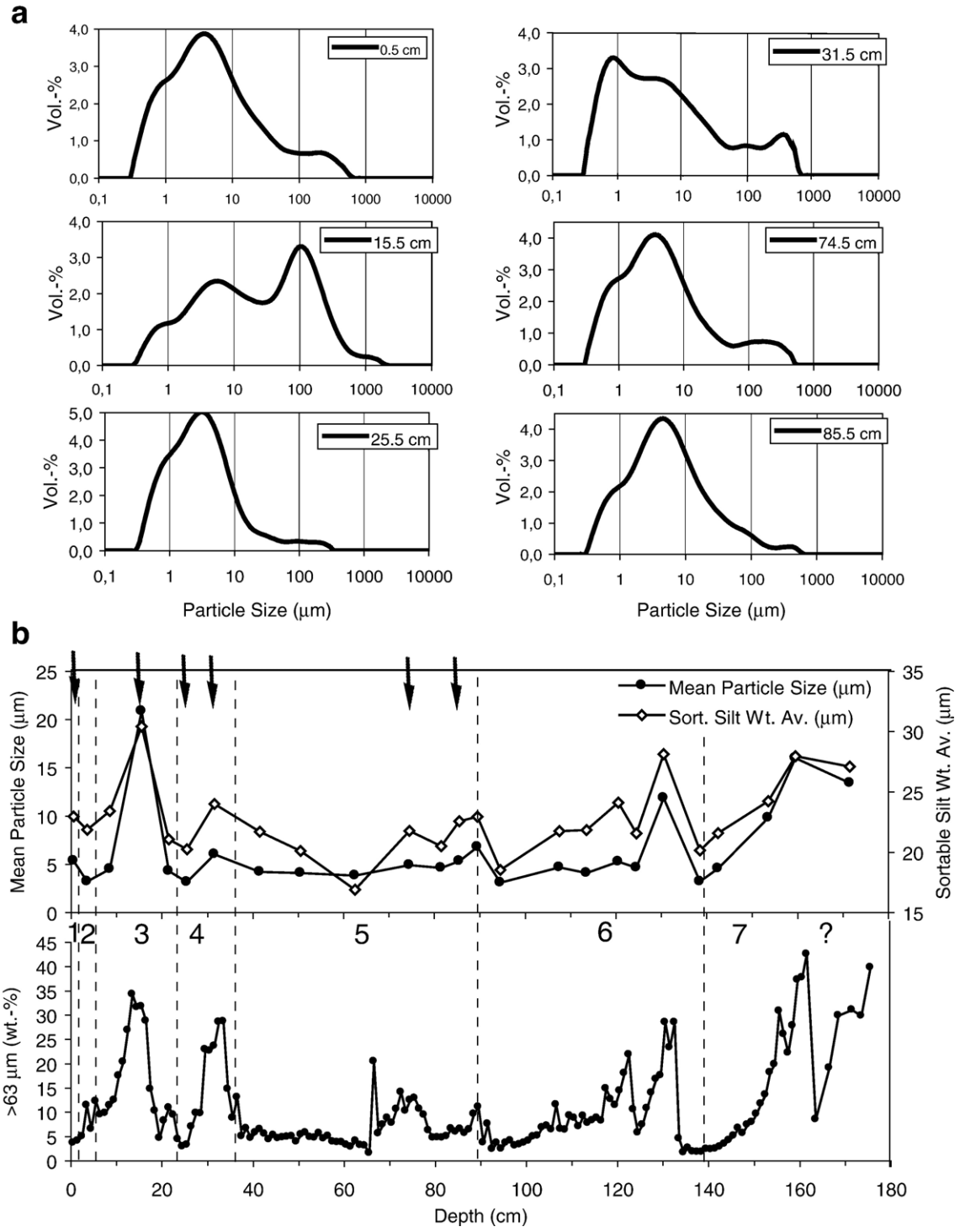


Fig. 4. Grain size records of GreenICE core 10 based on detailed laser particle size measurements. (a) Examples of different particle size distribution plots from sample levels: 0.5 cm (fine-grained mud, Holocene); 15.5 cm (sorting in fine sand mode, MIS 3); 25.5 cm (fine silt rich in detrital carbonate, MIS 4/3 transition); 31.5 cm (IRD rich, MIS 4); 74.5 cm (quite similar to Holocene sample, MIS 5d); 85.5 cm (fine-grained mud, MIS 5e). (b) Record of mean particle size and sortable silt weighted average. For comparison, the >63 µm (wt.%) record based on wet sieving, is shown below.

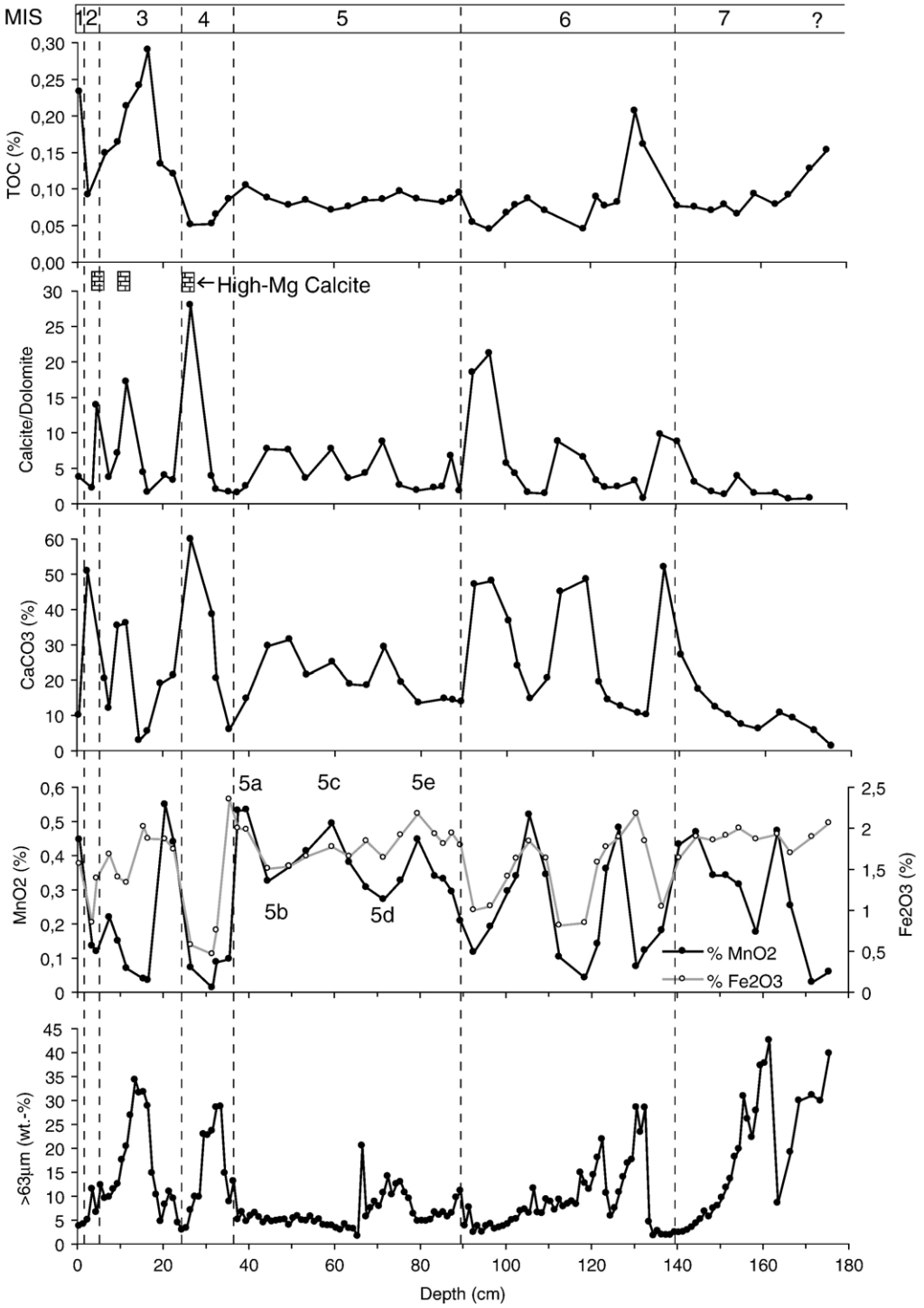


Fig. 5. GreenICE 10 geochemical and mineralogical data. From below, the fraction >63 µm, MnO_2 and Fe_2O_3 content, $CaCO_3$ content, calcite/dolomite ratio with levels enriched in high-Mg calcite indicated, and TOC content. The MnO_2 record may reveal single substages (e–a) within the MIS 5 section. However, the influence of detrital carbonate (CaCO3) with low absorptive properties, may limit the use of the Mn-record as a stratigraphical tool at this site.

light-coloured $CaCO_3$-rich units whereas high values characterise the dark brown units. Subtle colour changes within the thick B3 unit (MIS 5) appear to be reflected by the MnO_2 content. The Fe_2O_3 values to a large degree mimic the variability pattern of MnO_2. However, in the MIS 3 and MIS 7 sections, Fe_2O_3 content is relatively high, whereas MnO_2 show larger variability. It is evident that there is a strong inverse relationship between the MnO_2/Fe_2O_3 content and the $CaCO_3$ content. The manganese content thus reaches minimum contents in the light-coloured units characterised by peak $CaCO_3$ contents. Apart from glacial-interglacial changes in bottom water ventilation rates and manganese supply (cf. Jakobsson et al., 2000), this can be explained by the geochemical behaviour of manganese and iron that tend to concentrate in clay mineral-rich muds with high absorptive properties as opposed to sediments enriched in detrital carbonate material.

4.5. $CaCO_3$, TOC, and carbonate mineralogy

Bulk sediment calcium carbonate content is very high in core 10 (Fig. 5)), compared to other published data sets from the Arctic Ocean (Darby et al., 1989; Vogt, 1996; Vogt, 1997). The dark brown units (B1-B6) contain 5–15% $CaCO_3$. The fine-grained, light coloured units are characterised by peak values of 40–60% $CaCO_3$, whereas the more coarse-grained parts of the light-coloured units show considerably lower carbonate contents (5–15%). In the basal part of the core (L6), carbonate contents decrease to below 5%. TOC content is in general very low, with most values about 0.1%. Maximum TOC contents of about 0.2–0.3% are noted in two coarse fraction peaks at about 15–18 cm and 130–132; the two single units showing indication of bottom current sorting.

XRD results reveal that the carbonate material is dominated by calcite. Calcite/ dolomite ratios show a large variability (average 5.3), showing peak values above 10 in the fine-grained $CaCO_3$-rich intervals. Litho-units L3 and L2 (corresponding to MIS 4 and late MIS 3 and MIS 2) appear to be dominated by high-Mg calcite, with subordinary low-Mg calcite and dolomite (including Fe-rich dolomite) (Fig. 5). Calcite in litho-units L5-L3, on the other hand, is mainly composed of low-Mg calcite.

5. Discussion

5.1. Stratigraphic framework

The cyclic sequence of brown and light yellowish to gray beds in GreenICE core 10 reflects a succession of interglacial/interstadial and glacial beds. Similar cyclic successions are known from other parts of the Arctic Ocean (e.g. Mudie and Blasco, 1985; Phillips and Grantz, 1997; Spielhagen et al., 1997; Jakobsson et al., 2000; Polyak et al., 2004; Spielhagen et al., 2004). However, especially the glacial type beds show marked differences between different parts of the Arctic Ocean, reflecting different source areas, extension of circum-Arctic glaciations and sediment transport modes. The chronostratigraphic framework for late Quaternary interior Arctic Ocean records has recently been revised, and it has been shown that average hemipelagic sedimentation rates over some parts of the interior Arctic Ocean have been cm/kyr rather than mm/kyr (Backman et al., 2004; Spielhagen et al., 2004). This implies that marine isotope substage events can be identified in a number of key records allowing more detailed inter-core correlation and reconstruction of events. We use elements of this new chronostratigraphic framework as a basis for discussing specific events in the GreenICE record.

5.2. Planktic foraminifera abundance and isotope records

Well-preserved tests of planktic and benthic foraminifera occur almost throughout GreenICE core 10. Planktic foraminifera abundance peaks are associated with dark brown, Mn-enriched layers of stages 5, 3, and 1 (Figs. 2, 5). Minor peaks are also found within brown units of stage 7 and 6. Similar peaks of planktic foraminifera have been found in records on central Lomonosov Ridge (Nørgaard-Pedersen et al., 1998; Spielhagen et al., 2004), Alpha Ridge (Scott et al., 1989), Mendeleev Ridge (Polyak et al., 2004), Morris Jesup Rise (Nørgaard-Pedersen et al., 1998; Spielhagen et al., 2004), and Northwind Ridge (Poore et al., 1993). In general, the high planktic foraminifera abundance associated with fine-grained sediments indicate interglacial/interstadial periods with a restricted sea ice cover and open water leads during summer. However, due to the diluting effect of the dominant terrigenous material flux, the faunal abundance cannot alone be taken as a proxy for planktic productivity and sea–ice conditions. Nørgaard-Pedersen et al. (2007) found high percentages of small (63–125 μm) subpolar foraminifera *T. quinqueloba* associated with last interglacial (MIS 5e) and substage 5a sediments in GreenICE cores 11 and 10. The faunal assemblages are quite similar to those found present day at the summer ice margin of the Eurasian Basin, where Atlantic Water is advected to the Arctic Ocean. These data imply relatively reduced ice conditions north of Greenland during the last interglacial period. In the following we will present additional isotope data in support of this interpretation.

A comparison of the GreenICE core 10 *N. pachyderma* (s) $\delta^{18}O$ and $\delta^{13}C$ record to three key cores from the Morris Jesup Rise (PS2200), Alpha Ridge-Mendeleev Ridge junction (PS51/38-4), and Mendeleev Ridge (NP26), reveal both regional differences as well as similar trends of the MIS 7-1 isotope records (Fig. 6). The average $\delta^{18}O$ values become lighter along the transect from the Eurasian Basin PS2200 site to the distant Amerasian Basin site (NP26). This is explained by the higher freshwater and Pacific Water content of halocline waters in the Amerasian Basin (Beaufort Gyre system). Large excursions of $\delta^{18}O$ occur not only at oxygen isotope stage transitions, but also within stages. Some of these excursions seem to be a robust phenomenon in several, if not all of the records. E.g., a conspicuous increase in $\delta^{18}O$ and $\delta^{13}C$ values is observed in the middle part of the MIS 5 records. Such abrupt increases in $\delta^{18}O$ and $\delta^{13}C$ values, also observed within the MIS 4-3 sections, were suggested by Polyak et al. (2004) to represent a shift in the halocline structure, caused by global sea level decrease and cut off of Bering Strait low-salinity Pacific Water supply to the Amerasian Basin halocline layer. The Bering Strait is only about 50 m deep, and the global sea level record (Lea et al., 2002), reveals that a reduction in Pacific Water influence during the last glacial cycle should be most pronounced during MIS 5d, 5b, and at the stage 5/4 transition. During most of stages 4-2, the Bering Strait threshold did not allow Pacific Water to enter the Arctic Ocean.

The *T. quinqueloba* and *N. pachyderma* (s) $\delta^{18}O$ values of the MIS 5e stratigraphic level give very similar results (Fig. 3). Indeed, this supports the assumption of Nørgaard-Pedersen et al. (2007) that the *T. quinqueloba* specimens in the last interglacial section represent an interior Arctic Ocean local production reflecting interior Arctic Ocean halocline properties. Present day $\delta^{18}O$ values of living *T. quinqueloba* from the water column

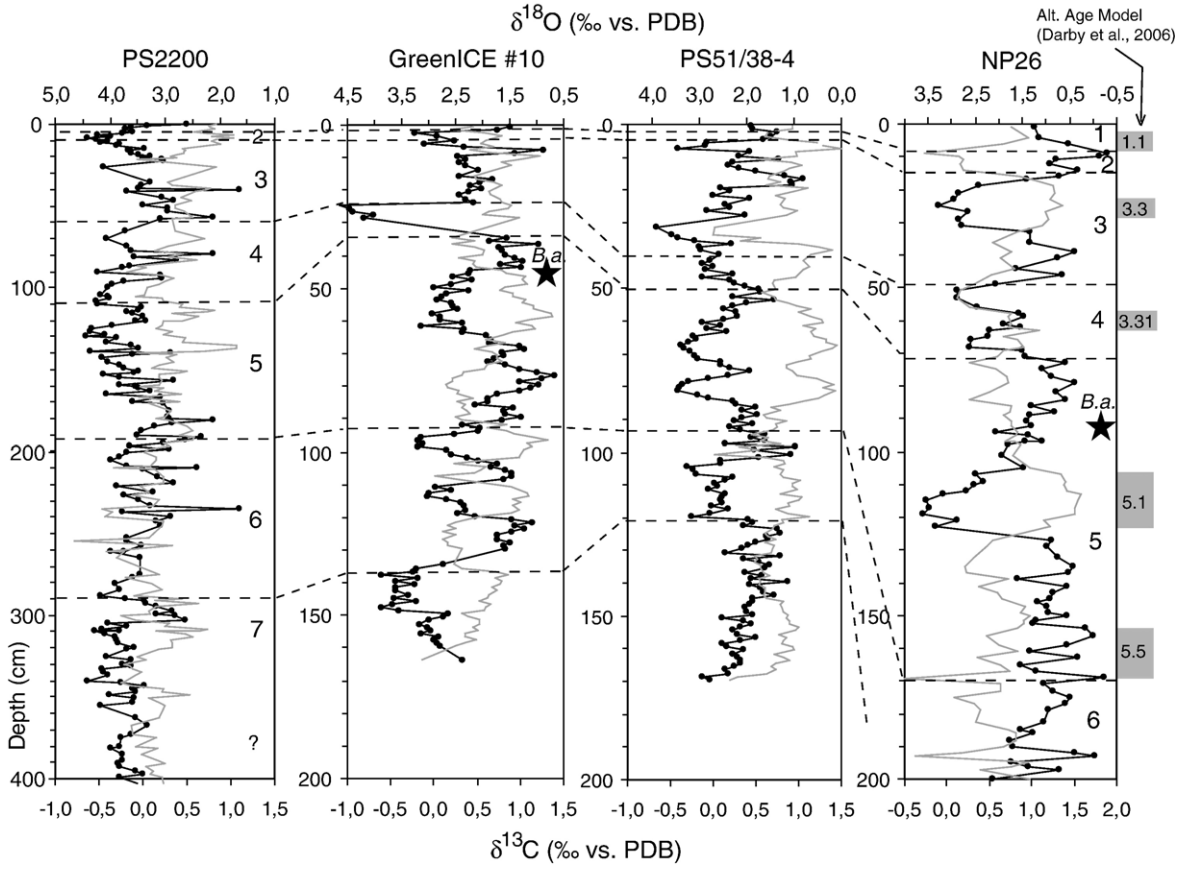


Fig. 6. Correlation of GreenICE core 10 *N. pachyderma* (s) $\delta^{18}O$ and $\delta^{13}C$ record to three key isotope records from the Morris Jesup Rise (PS2200: Spielhagen et al., 2004), Alpha Ridge-Mendeleev Ridge junction (PS51/38-4: Spielhagen et al., 2004), and Mendeleev Ridge (NP26: Polyak et al., 2004; Darby et al., 2006). The MIS subdivision of NP26 is based on this study. Stars indicate stratigraphic *zone of B. aculeata*. An alternative age model (substage isotope events) of NP26, given by Darby et al. (2006), is shown to the right of NP26.

of the eastern Fram Strait (charaterised by Atlantic water advection) are about 3.0–3.5‰ which is close to $\delta^{18}O$ values of *N. pachyderma* (s) from the same area (Volkmann and Mensch, 2001). We are not aware of last interglacial *T. quinqueloba* isotopic records from eastern Fram Strait. Many last interglacial and Holocene sections in that region appear to be severely influenced by carbonate dissolution (Knies et al., 2000; Wollenburg et al., 2001; Matthiessen et al., 2001). However, high-resolution *N. pachyderma* (s) isotope records from this area (Knies et al., 2000; Hald et al., 2001) show last interglacial $\delta^{18}O$ values in the range 2.7–3.5‰. The much lower last interglacial *T. quinqueloba* $\delta^{18}O$ values in the study area north of Greenland support that the subpolar specimens were not advected from the Fram Strait area, and likely represent a locally produced assemblage.

5.3. The glacial record

5.3.1. IRD events, correlation and glacial history

During the last glacial maximum, the Innuitian Ice Sheet over the NE Canadian archipelago coalesced with the Greenland Ice Sheet along the Nares Strait and with the Laurentide Ice Sheet to the south (England, 1999; England et al., 2006). The Innuitian Ice Sheet probably built to its maximum as late as 19 ^{14}C ka (England et al., 2006); a few millennia later that the much larger Laurentide Ice Sheet, culminating about 24–20 ^{14}C ka (Dyke et al., 2002). Two major ice streams along Nansen Fjord west of Ellesmere Island and along a channel west of Axel Heiberg Island drained the Innuitian Ice sheet to the Arctic Ocean. The margin of the ice sheet possibly lay to the north of the present coast (England et al., 2006). Ice streams from the Innuitian Ice sheet as well as a Nares Strait Greenland/Innuitian ice stream may have been important local sources for icebergs and sediment rafting near the GreenICE study area.

Beyond the last glacial maximum, very little is known about the extension of ice sheets in Arctic Canada and northern Greenland. To the west of the Innuitian Ice Sheet, large ice streams of the Laurentide Ice Sheet drained via inter-island troughs to the Arctic Ocean continental margin (Dyke and Prest, 1987; Dyke et al., 2002; Stokes et al., 2006). Sediment-core data from the Chukchi margin (ramp to the Northwind Ridge) confirm the existence of glacial erosion down to 450 m during the LGM and down to 750 m during an older glacial advance (tentatively placed between MIS 4 and 5d) (Polyak et al., 2007). The GreenICE core from adjacent to the continental margin shows a stratigraphically well-constrained record of the last two glacial-interglacial cycles that can assist in identifying past periods of major regional glacial activity in this area.

The GreenICE cores indicate enhanced deposition of coarse ice-rafted debris during the MIS 8/7 transition, periods of MIS 6, MIS 6/5 transition, MIS 5d, MIS 4, and late MIS 3 (30-40 14C ka). IRD deposition in the MIS 2 interval, however, appears to have been limited. In general the IRD composition enriched in detrital carbonates appears quite similar to other Amerasian Basin IRD records (Darby et al., 1989; Phillips and Grantz, 2001). However, as suggested in Section 5.3.2, the fine-grained detrital carbonate component may give additional clues to possible provenance areas.

The southernmost record of the Lomonosov Ridge, as represented by the GreenICE site, does not appear to contain the thick sandy, quartz-rich IRD units (MIS 6 and 4-3), reported from the central Lomonosov Ridge (Spielhagen et al., 1997; Jakobsson et al., 2001; Spielhagen et al., 2004). The sandy units can be traced to Morris Jesup Rise and Fram Strait in the Eurasia Basin, and to the Makarov Basin and the Alpha Ridge/Mendeleev Ridge junction in the Amerasia Basin (Spielhagen et al., 2004). From the eastern to the western (closer to the Canadian margin) part of the Alpha Ridge, the characteristic IRD units appear to thin out markedly (Minicucci and Clark, 1983) and, apparently, this is the case also from the central Lomonosov Ridge to its southern part north of Lincoln Sea. Abundant quart-rich IRD, on the other hand, is found in the basal part of GreenICE core 10, probably representing the MIS 8/7 transition. Due to the unknown downward extension of this IRD-rich section below the level recovered by GreenICE core 10, correlation to other key records appears problematic.

CESAR cores 102 and 103 from the Alpha ridge (Mudie and Blasco, 1985; Scott et al., 1989) show characteristic lithological units, faunal, and isotope data that, at least for the last two glacial-interglacial cycles, can be correlated to the GreenICE record (Fig. 7). Lithostratigraphic unit M (cf. Clark et al., 1980) in the CESAR cores, thus appears to correspond to MIS 5d-1 (i.e. the last glacial-interglacial cycle). Unit L appears to represent MIS 6-5e, the penultimate glacial cycle. The suggested correlation makes it possible to reinterpret the late Quaternary chronostratigraphy of the Alpha Ridge record (see Backman et al. (2004) for detailed discussion of Arctic Ocean magnetostratigraphy and chronostratigraphy).

Seismic records show possible glacial erosion and a very thin sediment cover of the top of the shallow (<550 m) and flat Lomonosov Ridge about 45 km from the GreenICE core site (Kristoffersen and Mikkelsen,

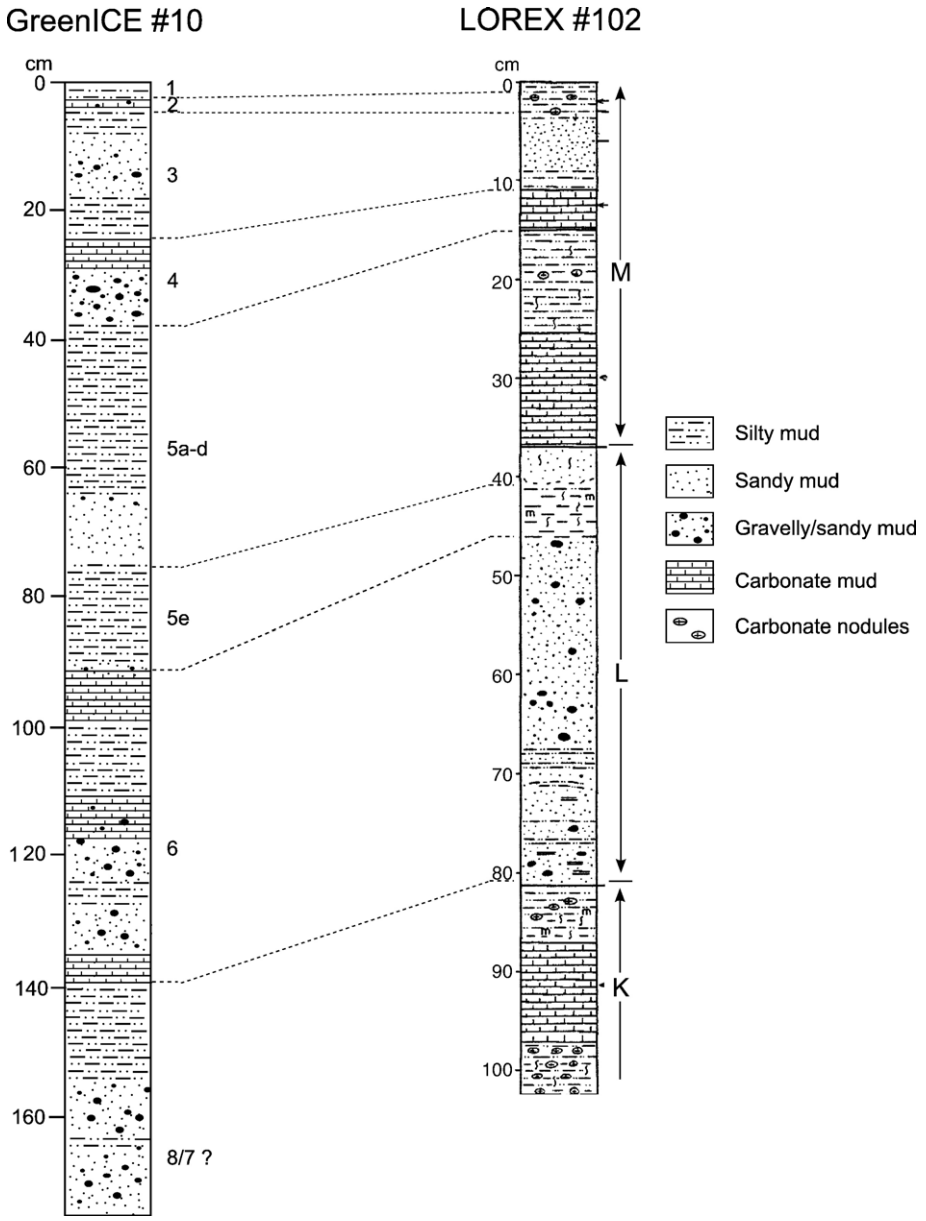


Fig. 7. Correlation of stratigrahic units in GreenICE core 10 (this study) and CESAR core 102 (Alpha Ridge: Scott et al., 1989). Isotope stages (MIS) are indicated to the right of GreenICE #10. Amerasian Basin litho-units (K-M) as defined by Clark et al. (1980) and given by Scott et al. (1989) are indicated to the right of CESAR #102.

2006). This erosion could either have taken place through a protruding ice shelf from the Lincoln Sea/Nares Strait or from deep draft ice bergs released to the Arctic Ocean (cf. Kristoffersen et al., 2004). Eroded sediment would probably have been redeposited as mass flows along the flanks of the bevelled ridge. There is no positive indication in the GreenICE record, though, supporting that such erosion and redeposition took place during the last two glacial-interglacial cycles. However, the circumstance that the GreenICE core 10 is from deeper water (>1000 m), and that the GreenICE cores nearer to the shallow ridge plateau are very short (or only sea floor surface samples (Nørgaard-Pedersen et al., 2007), limits the burden of proof for the timing of such erosion events.

5.3.2. Fine-grained detrital carbonate (DC) layers — deglaciation events?

The GreenICE record displays a number of light-coloured units with characteristic peaks in bulk carbonate

content reaching 40–60% (in the following called detrital carbonate (DC) layers). This appears to be the highest $CaCO_3$ contents reported from Quaternary Arctic Ocean sediment cores. The DC layers are almost barren in foraminifera, typically very fine-grained (very fine silt), and show in the MIS 4-2 section a high content of high-magnesium calcite. The majority of the fine-grained DC layers in GreenICE core 10 are superimposed on coarser-grained IRD units and followed by interglacial/interstadial type sediments. Thus it appears that the DC layers represent deposition associated with deglaciation periods (e.g. MIS 6/5 and 4/3 transitions).

Detrital carbonate-rich units and cycles are a characteristic phenomenon for Amerasia Basin Quaternary records. However, bulk carbonate contents in these cores in general show maximum contents of 20–30% (Darby et al., 1989). Moreover, Amerasia Basin $CaCO_3$ peaks are in general found in units also characterised by peak IRD contents. This IRD contains typically abundant dolomite, with only a subordinary amount of low-magnesium calcite (Darby et al., 1989; Phillips and Grantz, 2001). The dolomite-rich IRD can be traced back to large areas of Paleozoic platform carbonates cropping out in the Canadian Arctic (Darby et al., 1989; Bischof and Darby, 1999; Phillips and Grantz, 2001). North of Greenland, Morris Jesup Rise core PS2200 has revealed peaks of carbonate content of 20–30% (Vogt, 1997). These are by far the highest carbonate contents in Quaternary cores from the Eurasian Basin, where siliceous IRD material otherwise dominate Quaternary records (Vogt, 1996, 1997; Nørgaard-Pedersen et al., 1998; Phillips and Grantz, 2001). Apart from dolomite IRD, units enriched in high-magnesium calcite occur in the MIS 5-2 section (uppermost 2 m) of PS2200 (Vogt 1997; revised age model in Spielhagen et al., 2004).

In the northwest Labrador Sea, fine-grained DC layers of variable dolomitic/calcitic composition are a common feature at ice-proximal sites of the former NE Laurentide ice sheet. The carbonate layers appear to be associated with more distal Heinrich events (Andrews et al., 1998). The carbonate material probably represent 'rain out' of fine-grained particles from either overflow plumes or nepheloid layers (Hesse and Khodabakhsh, 1998; Rashid et al., 2003). Turbid surface plumes rich in fine-grained sediments are a well-known phenomenon of modern tide-water glaciers, but extend only for a limited distance, generally <10 km seawards from the ice margin (Elverhøi, 1984; Stewart, 1991). This is mainly because clay-rich fine-grained sediments tend to flocculate and form larger aggregates when they come in contact with seawater, and thus settle rapidly. Fine-grained carbonate particles, on the other hand, flocculate much less than clay minerals because of their lower electrical surface charges. Glacial-flour carbonate can thus stay in suspension considerably longer and therefore drift much further than clays when entrained by surface or mid-depth currents. Hesse et al. (1999) suggested that fine-grained detrital carbonate material found on the upper Labrador Slope in this way was transported about 200 km down-current from the ice-margin source.

Analogous to the depositional models for Labrador Sea continental margin DC layers, we suggest that the conspicuous DC layers in the GreenICE records represent proximal plume or nepheloid layer deposits. We may ask why the fine-grained detrital carbonate units in the GreenICE cores are mainly found at the transition between glacial and interglacial/interstadial units. First, with increasing temperatures at glacial-interglacial transitions, meltwater transport of fines to the sea was probably increasing. Secondly, the Atlantic Water boundary current system along the continental margin, was probably gaining in strength in connection to a better communication with the Nordic Seas (Hald et al., 2001; Wollenburg et al., 2001; Birgel and Hass, 2004). Thereby, fine grained carbonate material could be transported along the adjacent continental margin as e.g. nepheloid flows for long distances. Present day, it has been inferred that a cell of Atlantic Water detaches from the continental margin current system north of Ellesmere Island, and flows along the southern Lomonosov Ridge towards the north (Rudels et al., 1999; Kristoffersen and Mikkelsen, 2006). Similar subsurface currents could have brought large volumes of fine-grained detrial carbonate material to the GreenICE site during deglaciation events. The characteristic high-magnesium calcite content of the DC-layers from MIS 4-2, supports that the main sediment sources should possibly be found on Ellesmere Island or northern Greenland (cf. Vogt, 1997). Thus, Krawitz (1982) traced large abundances of fine-grained carbonate material from proximal glacier outlet regions of Ellesmere Island and NW Greenland to surface sediments of Kane Basin in the Nares Strait.

6. Conclusions

GreenICE core 10 contains a dominant hemipelagic record of cyclical glacial-interglacial changes encompassing MIS 7-1. On basis of biostratigraphic events and planktic foraminifera abundance and isotope records, it can be correlated to other key Arctic Ocean records.

The isotope record of *N. pachyderma* (s) show large similarities to Arctic Ocean key records. This supports

the over-regional character of the isotopic changes, likely reflecting major changes of freshwater flux to the Arctic Ocean halocline. Conspicuous high $\delta^{18}O$ values during periods of lowering of sea level (e.g. MIS 5d-5b, MIS 4) may be related to shut down of Pacific Water flow to the Arctic Ocean via the shallow Bering Strait.

The $\delta^{18}O$ values of subpolar foraminifera *T. quinqueloba* and polar *N. pachyderma* (s) in the GreenICE last interglacial unit are very similar, and several ‰ lower than values expected for the eastern Fram Strait region. This support the interpretation that the abundant subpolar foraminifera represent a local production, related to warm interglacial conditions and probably a much reduced sea ice cover in the interior Arctic Ocean.

Manganese peaks in Arctic Ocean sediments cores appear to be associated with warm interglacial/interstadial periods. However, the prominent anti-correlation with the bulk carbonate content (with low absorptive properties) suggests that manganese content alone cannot be used as an independent stratigraphic tool in Arctic Ocean sediment cores with relatively high contents of detrital carbonate.

The GreenICE cores indicate enhanced deposition of coarse ice-rafted debris during the MIS8/7 transition, periods of MIS 6, MIS 6/5 transition, MIS 5d, MIS 4, and late MIS 3 (30–40 ^{14}C kyr BP). During MIS 2, only little IRD was deposited in this area. The IRD contains detrital carbonate material similar to other Amerasia Basin records. However, the occurrence of fine-grained detrital carbonate layers at glacial-interglacial transitions appears to be unique to this area. The elevated content of high-magnesium calcite in MIS 4-2 detrital carbonate layers indicates probably a provenance from Ellesmere Island or North Greenland. It is suggested, that the DC layers were deposited from nepheloid flows, during deglaciations of Ellesmere Island when the counter clockwise Atlantic Water boundary current was gaining strength along the continental margin.

Acknowledgements

We would like to thank all those that contributed with logistical assistance during the GreenICE field campaign in May 2004. Special thanks go to John Boserup (GEUS) for his technical assistance and hard work under difficult conditions. For assistance with laboratory analyses, we thank Ingerlise Nørgaard, Kirsten Fries, and Vibeke Ernstsen at GEUS. We thank also Dr. Christoph Vogt, ZEKAM Laboratory, University of Bremen, for XRD measurements and discussion of carbonate mineralogy. This contribution is a result of the EU GreenICE Project (No. EUK-2001-00280).

References

ACEX Shipboard Scientific Party, 2005. Arctic Coring Expedition (ACEX): paleoceanographic and tectonic evolution of the central Arctic Ocean. IODP Prel. Rep, p. 302. http://www.ecord.org/exp/acex/302PR.pdf.

Andrews, J.T., Kirby, M.E., Aksu, A., Barber, D., Meese, D., 1998. Late Quaternary detrital carbonate (DC) layers in Baffin Bay marine sediments (67 °–74°): correlation with Heinrich events in the North Atlantic? Quat. Sci. Rev. 17, 1125–1137.

Backman, J., Jakobsson, M., Løvlie, R., Polyak, L., Febo, L.A., 2004. Is the Central Arctic Ocean a sediment starved basin? Quat. Sci. Rev. 23 (11–13), 1435–1454.

Birgel, D., Hass, H.C., 2004. Oceanic and atmospheric variations during the last deglaciation in the Fram Strait (Arctic Ocean): a coupled high-resolution organochemical and sedimentological study. Quat. Sci. Rev. 23, 29–47.

Bischof, J., Darby, D., 1999. Quaternary ice transport in the Candian Arctic and extent of Late Wisconsinan glaciation in the Queen Elizabeth Islands. Can. J. Earth Sci. 36, 2007–2022.

Chung, F.H., 1974. Quantitative interpretation of X-ray diffraction patterns, I. Matrix-flushing method of quantitative multicomponent analysis. J. Appl. Crystallogr. 7, 513–519.

Clark, D., Hanson, A., 1983. Central Arctic Ocean sediment texture: a key to ice transport mechanisms. In: Molnia, B.F. (Ed.), Glacial-marine Sedimentation. Plenum Press, New York, pp. 301–330.

Clark, D.L., Whitman, R.R., Morgan, K.A., Mackey, S.D., 1980. Stratigraphy and glacial-marine sediments of the Amerasian Basin, central Arctic Ocean. Geol. Soc. Am. Spec. Paper, vol. 181, p. 57.

Darby, D.A., Naidu, A.S., Mowatt, T.C., Jones, G., 1989. Sediment composition and sedimentary processes in the Arctic Ocean. In: Herman, Y. (Ed.), The Arctic Seas—climatology, oceanography, geology, and biology. Van Nostrand Reinhold Co., New York, pp. 657–720.

Darby, D.A., Polyak, L., Bauch, H.A., 2006. Past glacial and interglacial conditions in the Arctic Ocean and marginal seas — a review. Progr. Oceanogr. 71, 129–144.

Dyke, A.S., Prest, V.K., 1987. Late Wisconsinan and Holocene history of the Larentide Ice Sheet. Geogr. Phys. Quat. 41, 237–263.

Dyke, A.S., Andrews, J.T., Clark, P.U., England, J.H., Miller, G.H., Shaw, J., Veillette, J.J., 2002. The Laurentide and Innuitian ice sheets during the Last Glacial Maximum. Quat. Sci. Rev. 21, 9–31.

Elverhøi, A., 1984. Glacigenic and associated marine sediments in the Weddell Sea, fiords of Spitsbergen and the Barents Sea: a review. Mar. Geol. 57, 53–88.

England, J., 1999. Coalescent Greenland and Innuitian ice during the Last Glacial Maximum: revising the Quaternary of the Canadian High Arctic. Quat. Sci. Rev. 18, 421–556.

England, J., Atkinson, N., Bednarski, J., Dyke, A.S., Hodgson, D.A., Ó Cofaigh, C., 2006. The Innuitian Ice Sheet: configuration, dynamics and chronology. Quat. Sci. Rev. 25 (7–8), 689–703.

Funder, J., Hansen, L., 1996. The Greenland ice sheet — a model for its culmination and decay during and after the last glacial maximum. Bull. Geol. Soc. Den. 42, 137–152.

Gard, G., 1988. Late Quaternary calcareous nannofossil biozonation, chronology and palaeo-oceanography in areas north of the Faeroe-Iceland Ridge. Quat. Sci. Rev. 7, 65–78.

Gard, G., Backman, J., 1990. Synthesis of Arctic and Sub-Arctic coccolith biochronology and history of North Atlantic Drift water influx during the last 500,000 years. In: Bleil, U., Thiede, J. (Eds.), Geological History of the Polar Oceans: Arctic versus Antarctic.

NATO ASI Series C, vol. 308. Kluwer Academic Publishers, Dordrecht, pp. 417–436.

Haas, C., Hendricks, S., Doble, M., 2006. Comparison of the sea ice thickness distribution in the Lincoln Sea and adjacent Arctic Ocean in 2004 and 2005. Ann. Glaciol. 44, 247–252.

Hald, M., Dokken, T., Mikalsen, G., 2001. Abrupt climatic change during the last interglacial-glacial cycle in the polar North Atlantic. Mar. Geol. 176, 121–137.

Hesse, R., Khodabakhsh, S., 1998. Depositional facies of late Pleistocene Heinrich events in the Labrador Sea. Geology 26 (2), 103–106.

Hesse, R., Klauck, I., Khodabakhsh, S., Piper, D., 1999. Continental slope sedimentation adjacent to an ice margin. III. The upper Labrador Slope. Mar. Geol. 155, 249–276.

Jakobsson, M., Løvlie, R., Al-Hanbali, H., Arnold, E., Backman, J., Mörth, M., 2000. Manganese and color cycles in Arctic Ocean sediments constrain Pleistocene chronology. Geology 28 (1), 23–26.

Jakobsson, M., Løvlie, R., Arnold, E., Backman, J., Polyak, L., Knutsen, L., Musatov, E., 2001. Pleistocene stratigraphy and paleoenvironmental variation from Lomonosov Ridge sediments, central Arctic Ocean. Glob. Planet. Change 31, 1–21.

Knies, J., Nowaczyk, N., Müller, C., Vogt, C., Stein, R., 2000. A multiproxy approach to reconstruct the environmental changes along the Eurasian continental margin over the last 150,000 years. Mar. Geol. 163, 317–344.

Krawitz, J.-H., 1982. The <2 μm fraction of some high Arctic glacial and glacial-marine sediments. In: Embry, A.F., Balkwill, H.R. (Eds.), Arctic Geology and Geophysics: Proceedings of the Third International Symposium on Arctic Geology. Canadian Society of Petroleum Geologists, Calgary, pp. 297–307.

Kristoffersen, Y., Mikkelsen, N., 2006. On sediment deposition and nature of the plate boundary at the junction between the submarine Lomonosov Ridge, Arctic Ocean and the continental margin of Arctic Canada/North Greenland. Mar. Geol. 225, 265–278.

Kristoffersen, Y., Coakley, B., Jokat, W., Edwards, M., Brekke, H., Gjengedal, J., 2004. Seabed erosion on the Lomonosov Ridge, central Arctic Ocean: a tale of deep draft icebergs in the Eurasia basin and the influence of Atlantic water inflow on iceberg motion? Paleoceanography 19, PA3006. doi:10.1029/2003PA000985.

Lea, D.A., Martin, P.A., Pak, D.K., Spero, H., 2002. Reconstructing a 350 ky history of sea level using planktonic Mg/Ca and oxygen isotope records from a Cocos Ridge core. Quat. Sci. Rev. 21, 283–293.

Matthiessen, J., Knies, J., Nowaczyk, N.R., Stein, R., 2001. Late Quaternary dinoflagellate cyst stratigraphy at the Eurasian continental margin, Arctic Ocean: indications for Atlantic waterinflow in the past 150,000 years. Glob. Planet. Change 31 (1–4), 65–86.

McCave, I.N., Manighetti, B., Robinson, S.O., 1995. Sortable silt and sediment size/composition slicing: parameters for paleocurrent speed and paleoceanography. Paleoceanography 10, 593–610.

Mehra, O.P., Jackson, M.L., 1960. Iron oxide removal from soils and clays by dithionite citrate system buffered with sodium bicarbonate. Clays Clay Miner. 5, 317–327.

Minicucci, D.A., Clark, D.L., 1983. A Late Cenozoic stratigraphy for glacial-marine sediments of the eastern Alpha Cordillera, central Arctic Ocean. In: Molnia, B.F. (Ed.), Glacial-marine sedimentation. Plenum Press, New York, pp. 331–365.

Mudie, P.J., Blasco, S.M., 1985. Lithostratigraphy of the CESAR cores. In: Jackson, H.R., Mudie, P.J., Blasco, S.M. (Eds.), Initial Geological Report on CESAR — the Canadian Expedition to Study the Alpha Ridge, Arctic Ocean. Geol. Surv. Canada, Paper, vol. 84-22, pp. 59–99.

Nørgaard-Pedersen, N., Spielhagen, R.F., Thiede, J., Kassens, H., 1998. Central Arctic surface ocean environment during the past 80,000 years. Paleoceanography 13 (2), 193–1204.

Nørgaard-Pedersen, N., Spielhagen, R.F., Erlenkeuser, H., Grootes, P., Heinemeier, J., Knies, J., 2003. The Arctic Ocean during the Last Glacial Maximum: Atlantic and Polar domains of surface water mass distribution and ice cover. Paleoceanography 18 (3), 1063. doi:10.1029/2002PA000781.

Nørgaard-Pedersen, N., Mikkelsen, N., Lassen, S.J., Kristoffersen, Y., Sheldon, E., 2007. Reduced sea ice concentrations in the Arctic Ocean during the last interglacial period revealed by sediment cores off northern Greenland. Paleoceanography 22, PA1218. doi:10.1029/2006PA001283.

Phillips, R.L., Grantz, A., 1997. Quaternary history of sea ice and paleoclimate in the Amerasia basin, Arctic Ocean, as recorded in the cyclical strata of Northwind Ridge. Geol. Soc. Amer. Bull. 109, 1101–1115.

Phillips, R.L., Grantz, A., 2001. Regional variations in provenance and abundance of ice-rafted clasts in Arctic Ocean sediments: implications for the configuration of Late Quaternary oceanic and atmospheric circulation in the Arctic. Mar. Geol. 172, 91–115.

Polyak, L., Curry, W.B., Darby, D.A., Bischof, J., Cronin, T.M., 2004. Contrasting glacial/interglacial regimes in the western Arctic Ocean as exemplified by a sedimentary record from the Mendeleev Ridge. Palaeogeogr., Palaeoclimatol. Palaeoecol. 20, 73–93.

Polyak, L., Darby, D.A., Bischof, J.F., Jakobsson, M., 2007. Stratigraphic constraints on late Pleistocene glacial erosion and deglaciation of the Chukchi margin, Arctic Ocean. Quat. Res. 67 (2), 234–245.

Poore, R.Z., Phillips, R.L., Rieck, H.J., 1993. Paleoclimate record for Northwind Ridge, western Arctic Ocean. Paleoceanography 8, 149–159.

Poore, R.Z., Ishman, S.E., Phillips, R.L., McNeil, D., 1994. Quaternary stratigraphy andpaleoceanography of the Canada Basin, western Arctic Ocean. USGS Bull. 2080, 1–32.

Rashid, H., Hesse, R., Piper, J.W., 2003. Origin of unusually thick Heinrich layers in ice-proximal regions of the northwest Labrador Sea. Earth Planet. Sci. Lett. 208, 319–336.

Rudels, B., Friederich, H.J., Quadfasel, D., 1999. The Arctic circumpolar boundary current. Deep-Sea Res. II 46, 1023–1062.

Scott, D.B., Mudie, P.J., Baki, V., MacKinnon, K.D., Cole, F.E., 1989. Biostratigraphy and Late Cenozoic paleoceanography of the Arctic Ocean: foraminiferal, lithostratigraphic, and isotopic evidence. Geol. Soc. Amer. Bull. 101, 260–277.

Simstich, J., Sarnthein, M., Erlenkeuser, H., 2003. Paired $\delta^{18}O$ signals of *Neogloboquadrina pachyderma* (s) and *Turborotalita quinqueloba* show thermal stratification structure in Nordic Seas. Mar. Micropaleontol. 48 (1–2), 107–125.

Spielhagen, R.F., Bonani, G., Eisenhauer, A., Frank, M., Frederichs, T., Kassens, H., Kubik, P.W., Nørgaard-Pedersen, N., Nowaczyk, N.R., Mangini, A., Schäper, S., Stein, R., Thiede, J., Tiedemann, R., Wahsner, M., 1997. Arctic Ocean evidence for Late Quaternary initiation of northern Eurasian ice sheets. Geology 25, 783–786.

Spielhagen, R.F., Baumann, K.-H., Erlenkeuser, H., Nowaczyk, N.R., Nørgaard-Pedersen, N., Vogt, C., Weiel, D., 2004. Arctic Ocean deep-sea record of northern Eurasian ice sheet history. Quat. Sci. Rev. 23, 1455–1483.

Stewart, T.G., 1991. Glacial-marine sedimentation from tidewater glaciers in the Canadian High Arctic. In: Anderson, J.B., Ashley, G.M. (Eds.), Glacial-Marine sedimentation: paleoclimatic significance. Geol. Soc. Am. Spec. Pap., vol. 261, pp. 95–105.

Stokes, C.R., Clark, C.D., Winsborrow, M.C.M., 2006. Subglacial bedform evidence for a major palaeo-ice stream and its retreat phases in Amundsen Golf, Canadian Arctic Archipelago. J. Quat. Sci. 21 (4), 399–412.

Thierstein, H.R., Geitzenauer, K., Molfino, B., Shackleton, N.J., 1977. Global synchroneity of late Quarternary coccolith datum levels: validation by oxygen isotopes. Geology 5, 400–404.

Vogt, C., 1996. Bulk mineralogy in surface sediments from the eastern central Arctic Ocean. In: Stein, R., Ivanov, G., Levitan, M., Fahl, K. (Eds.), Surface-sediment composition and sedimentary processes in the Central Arctic Ocean and along the Eurasian Continental Margin. . Berichte zur Polarforschung. AWI, Bremerhaven, pp. 159–171.

Vogt, C., 1997. Zeitliche und räumliche Verteilung von Mineralvergesellschaftungen in spat-quartären Sedimenten des Arktischen Ozeans und ihre Nutzbarkeit als Klimaindikatoren während der Glazial/Interglazial-Wechsel. Reports on Polar Research, vol. 251. AWI, Bremerhaven. 309 pp.

Volkmann, R., Mensch, M., 2001. Stable isotope composition ($\delta^{18}O$, $\delta^{13}C$) of living planktic foraminifers in the outer Laptev Sea and the Fram Strait. Mar. Micropaleontol. 42 (3), 163–188.

Wadhams, P., 1997. Ice thickness in the Arctic Ocean: the statistical reliability of experimental data. J. Geophys. Res. 102, 27951–27959.

Wadhams, P., Davis, N.R., 2000. Further evidence of ice thinning in the Arctic Ocean. Geophys. Res. Lett. 27, 3973–3975.

Wollenburg, J., Kuhnt, W., Mackensen, A., 2001. Changes in Arctic Ocean paleoproductivity and hydrography during the last 145 kyr: The benthic foraminiferal record. Paleoceanography 16 (1), 65–77.